Geomechanics and Engineering, *Vol. 33, No. 3 (2023) 243-259*
https://doi.org/10.12989/gae.2023.33.3.243

Combined resonant column and cyclic triaxial tests to estimate the dynamic behavior of undisturbed saturated clayey soils of Adapazarı, Turkey

Ersin Güler* and Kamil Bekir Afacan[a]

Eskisehir Osmangazi University, Civil Engineering Department, 26480, Turkey

(*Received October 21, 2022, Revised January 27, 2023, Accepted February 15, 2023*)

Abstract. Turkey is one of the most important earthquake regions in Europe. This region has been exposed to many earthquakes of different magnitudes from past to present. It is of great importance to determine the dynamic properties of the soils for structures to be built in earthquake zones. In order to minimize the damages that may occur, the behavior of the soils under repeated loads should be known and taken into consideration in the design. In this study, 4 different point borings were taken near active fault lines in the North Anatolian fault zone (NAFZ). In order to determine the dynamic parameters of soils, both dynamic triaxial (TRX) and resonant column (RC) tests were carried out on undisturbed samples at every 5 m. As a result of the experiments, V_s and G_{max} values were obtained from the field and differences were determined. The dynamic behavior of the soil was examined at varying depths with the comparison of reference models in the literature and compatible results were obtained. Finally, the behavior at the transition region is highlighted. As a result, three shear modulus and dumping ratio models have been proposed for clay soils to be used in different soil conditions.

Keywords: cyclic triaxial; dynamic properties; resonant column; undisturbed clay

1. Introduction

Soils and structures are subject to deformations due to repeated loads and they often control the design parameters. Therefore, evaluation of the dynamic behavior of soils under seismic loads is very crucial for geotechnical engineers. It has been widely studied in the literature and very recent ones focus on the dynamic behavior of different soils along with the liquefaction concept (Chattaraj and Sengupta 2016; Hussain and Sachan 2019; Thomas and Rangaswamy 2020). In order to estimate the stress-strain properties of in situ soils under cyclic loads, dynamic properties should be assessed first and then site-specific analyses can be conducted to predict the ground and superstructures' behaviors. Initial dynamic shear modulus-G_{max}; normalized dynamic shear modulus (G/ G_{max}); and damping ratio D values are needed to constitute the dynamic soil properties (Zhou *et al*. 2017, Bayat and Ghalandarzadeh 2018). These characteristics can be obtained both in the field and in the laboratory environment (Varghese *et al.* 2019). Various laboratory test sets are utilized to calculate the dynamic parameters of soils at different strain values. Dynamic triaxial (TRX) and resonant column (RC) experiments are used widely as recommended by ASTM D4015-15 and D4767-11 Standards. Shear strain level is the key parameter which test to run. RC tests are good for shear strains lower than 0.01%, whereas the TRX tests are for higher levels as presented in Fig. 1.

Two different test systems were used to obtain shear modulus strain curves of soils at both medium and small deformation levels. Regarding the RC test system, which is one of these experiments, researchers have carried out so many studies on different samples, under different conditions (Sexena and Reddy 1989, Kim *et al.* 2018, Kweon and Kim 2000, Park *et al.* 2015, Subramaniam and Banerjee 2016, Li and Senetakis 2018). Likewise, the TRX test system has been used in in the literature a lot (Kokusho 1980, Kumar and Krishna 2017, Sobolev and Ter-Martirosyan 2018, Jamali *et al.* 2018, Salem *et al.* 2018, Shivaprakash and Dinesh 2018) to estimate the dynamic behavior at higher strain levels in terms of different soils, confining pressures, loads, etc.

Another important point to obtain the dynamic properties of a soil is whether the sample is undisturbed or not. Since the parameters gathered from the site specific analyses will be used in the design of structures especially in earthquake zones, it is necessary to use undisturbed samples that reflect the site conditions the best. There are well known studies, such as Vucetic and Dobry (1991), Darendeli (2001), Amir-Faryar *et al.* (2016), that focused on the dynamic behavior of undisturbed samples and their reference models have been used in the practice extensively.

Experiments carried out to determine the behavior of soils under dynamic loads determine the shear modulus and damping ratio values of the soil at different deformation levels. Initial or maximum shear modulus can be calculated at very low strain levels and it may not be accurate depend on the sensitivity of the equipment. Measurement of shear wave velocity (V_s), one of the data reflecting the properties of the site, plays an important role in determining this value.

*Corresponding author, Ph.D.
E-mail: eguler@ogu.edu.tr
[a]Associate Professor
E-mail: kafacan@ogu.edu.tr

ISSN: 2005-307X (Print), 2092-6219 (Online)

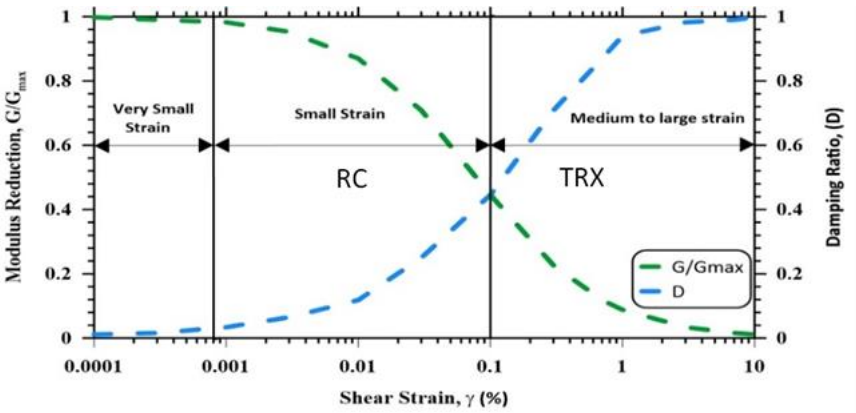

Fig. 1 A typical example of the modulus reduction and damping ratio curves

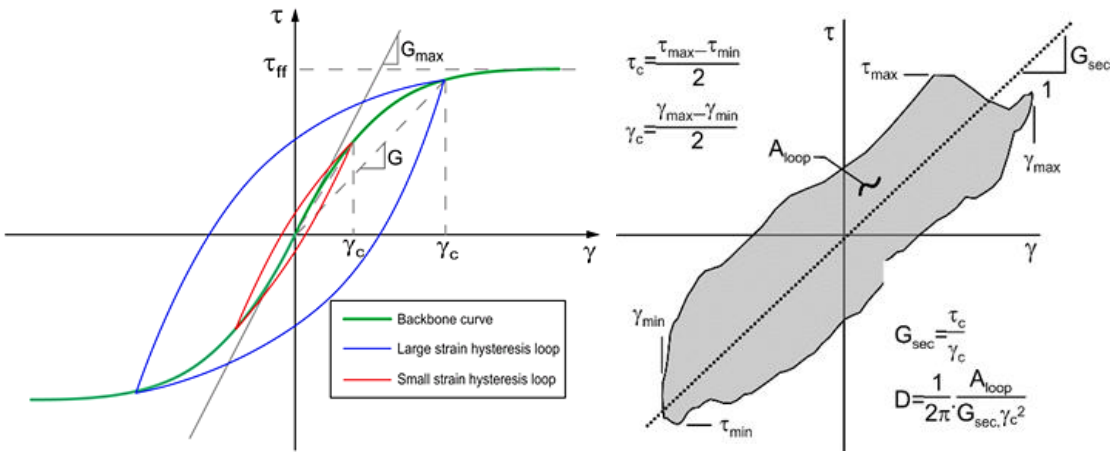

Fig. 2 Stress-strain curve of the soils (Stewart *et al*. 2014)

They are directly related to each other and maximum shear modulus can be calculated from the field shear wave velocity ($G_{max}=\rho.V_s^2$) across the soil layers of the studied area.

There are two main specifications to understand the behavior of soils under repeated loads: 1) stress-strain behavior over a wide range, 2) the soil rigidity. Stress-strain properties of soils are defined as changes in shear modulus and damping ratio values due to cyclic loading for different unit shear deformation levels. As a result of dynamic loading, a conventional loop that shows the stress-strain behavior change of the soil sample is presented in Fig. 2 (taken from Stewart *et al.* 2014) and it is basically called as the 'hysteresis loop'. These loops combine together and establish the backbone curve (Güler and Afacan 2021).

In order to carry out all these studies, it is necessary to carry out both field tests and laboratory tests in earthquake zones and to obtain important parameters in the design by combining the obtained data.

This study concentrates on the undisturbed soil samples taken from the Sakarya province located on the North Anatolian Fault Zone (NAFZ) and the area has been devastatingly affected by Kocaeli and Adapazari Earthquakes in 1999. The purpose of the research is to determine the dynamic properties of the undisturbed samples taken from different points close to the fault line employing the TRX and RC tests at every 5m. In addition, the shear wave velocity values from the in situ and laboratory will be compared. Finally, the obtained dynamic behavior of borings will be examined with the models widely used in the literature and new models will be proposed to the literature.

2. Geology and seismicity of the studied area

Turkey is one of most seismic region in Europe and surrounded by the North Anatolian Fault in the north and the East Anatolian Fault in the southeast region. Both active fault lines cause earthquakes today. Earthquakes of different depths and magnitude on and around fault lines are shown in Fig. 3. The North Anatolian fault does not have a single slip plane and consists of many parts. The fault line is in the state of a 'fault zone' with a width of 500-1000 m and it is a strike-slip and right-sided fault. Right-sided horizontal sliding movements prevail in all parts of the fault. At the same time, to a lesser extent, vertical movements were also manifested. It is known that the land to the north of the fault slides to the right and downwards. There is no exact information about when the North Anatolian fault formed geologically and how much sliding movement it has happened since its beginning to our time (Ketin 1991).

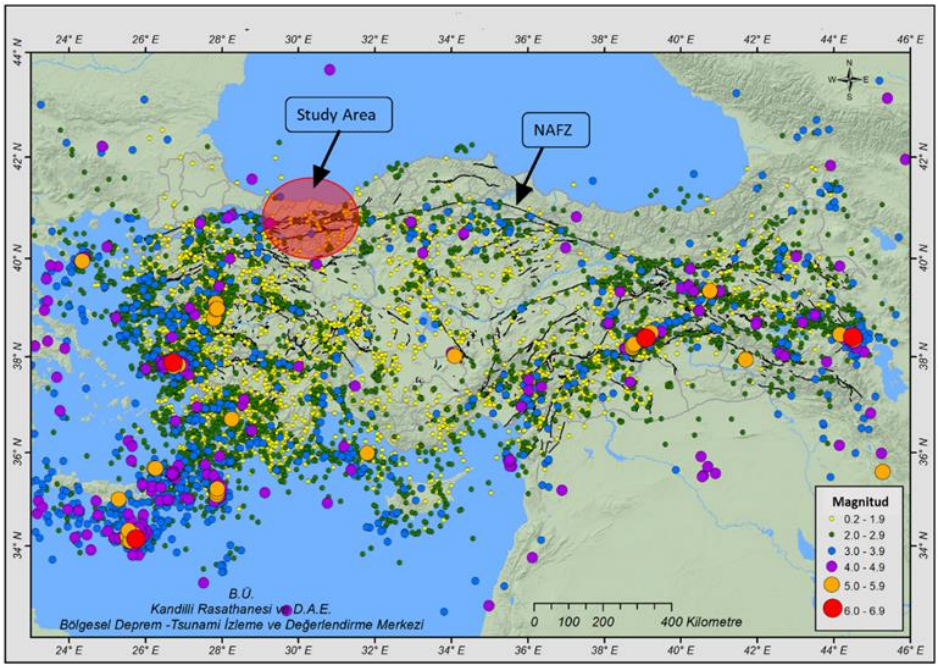

Fig. 3 Seismicity of the Turkey and study area (Boğaziçi University Kandilli Observatory and Earthquake Research Institute Regional Earthquake 2020)

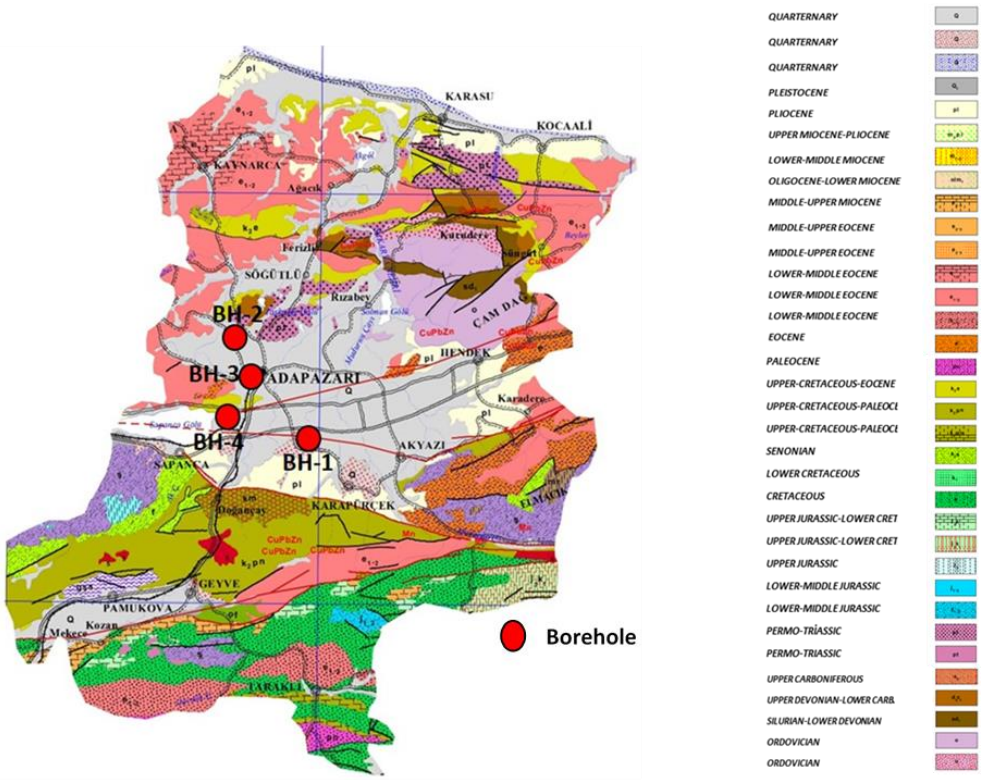

Fig. 4 Geology maps of study area (Akbaş *et al.* 2002).

Adapazari, which is the center of Sakarya province, has suffered great damage and loss of life in earthquakes in the past. Due to the presence of water-saturated deep alluvial layers in the region, it was observed that the damages increased with the effect of liquefaction and soil amplification during the earthquake. The region has attracted the attention of many researchers for academic research because it receives heavy rainfall throughout the year, has streams with deep alluvial layers, and is close to the active fault line (Kaya and Erken 2015, Harman 2016, Sakarya Governorship Provincial Directorate Of Environment And Urbanization 2018). Adapazarı plain is

Fig. 5 Drilling work at the BH-1 point

Fig. 6 (a) UD sample, (b) SPT tests and (c) Vs tests

represented by Quaternary (Q) widely in the area. A large part of the region is located on this alluvium and there are formations at different heights in the surrounding area (Fig. 4). During the borings performed by the General Directorate of State Water Works (DSI) at different times, bedrock was not found even at 200-300 m depths (Komazawa 2002, Bol 2003). Major damages and casualties occurred during the 1999 Kocaeli (M: 7.4) and Duzce (M: 7.2) earthquakes, and studies have showed that the main reasons were the soil amplification and the liquefaction.

The studied area is located on the North Anatolian Fault line, was severely damaged by previous earthquakes in the last century such as 1943 Hendek (M:6.6), 1957 Abant (M:7.1), 1967 Akyazı (M: 6.0), 1999 Adapazarı (M:7.2) Earthquakes (Komazawa 2002; Bol 2003; Harman 2016). The strike-slip segments of Sapanca-Gölcük, İzmit-Karamürsel and Yarımca-Yalova of the NAF zone played an important role in recent earthquakes (Ketin 1991). It is important to determine the dynamic properties of the soil for safer design of the buildings, as the region has advanced in the industry and is located in an active earthquake zone.

The borings and the geology of the area is presented in Fig. 4.

3. Field tests and taking of undisturbed samples

After examining the seismicity and geological situation of the region, studies were carried out at the drilling points in the Adapazarı district of Sakarya province shown in Fig. 3. Undisturbed samples were taken at every 5 m of boreholes and they were obtained at the depths determined with the help of UD tubes. Fig. 5 shows the field testing and Fig. 6(a) presents an example of UD tubes for undisturbed samples from 2.5, 7.5, 12.5 and 17.5 m depths. In addition, the samples between these UD tubes were taken with sample boxes and used for identification purposes.

Moreover, SPT tests were carried out at every 1.5 m at the drilling points, and the variation along the depth was obtained and samples were taken (Fig. 6(b)). Shear wave velocity was also measured at the points determined in the field, and its variation along the depth was obtained (Fig. 6(c)).

4. Test apparatuses and program

Dynamic Cyclic Triaxial Test (TRX), and Resonant

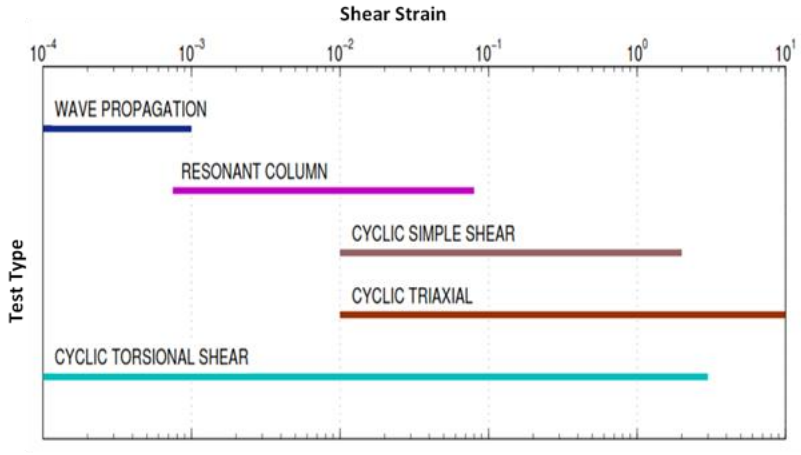

Fig. 7 Deformation range in dynamic laboratory tests (Houbrechts *et al*. 2011).

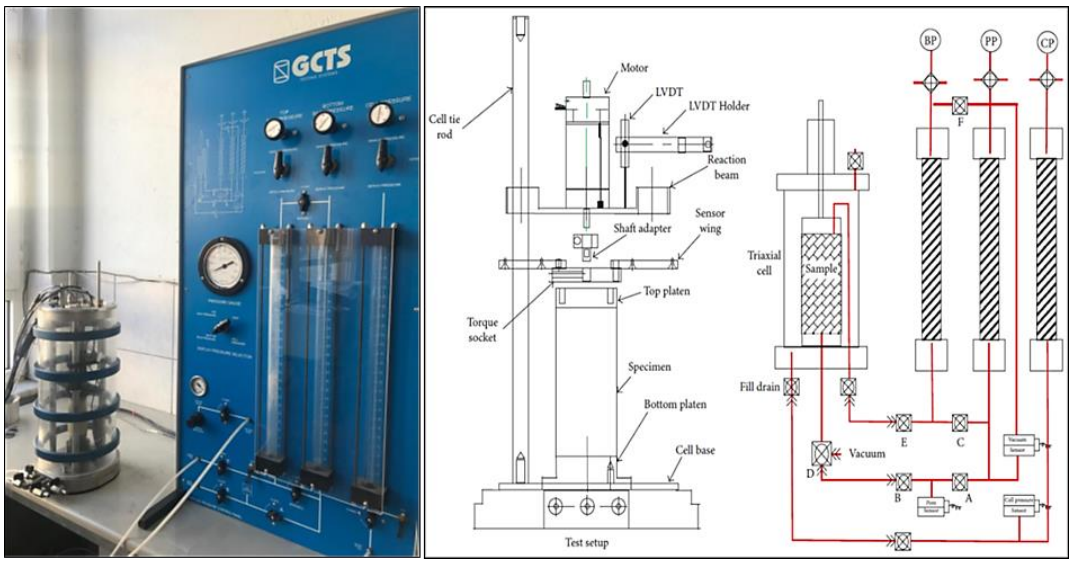

Fig. 8 Resonant column test system

Column Test (RC) were performed on the undisturbed fine grained soil samples. Experiments in this study were carried out with the CTX and RC test systems in the Soil Mechanics Laboratory of Eskişehir Osmangazi University. The most important differences between laboratory experiments is the deformation levels that one can reach and Fig. 7 underlines these levels for varying dynamic tests.

As seen in the figure, resonant column and cyclic triaxial tests are solely not enough to establish a dynamic behavior of soil at varying strains. The idea of the study is to obtain a data sets that combine the test results to get the behavior in a wider range.

The experiments in this study were performed according to ASTM D 4015 and ASTM D 3999 standards. The target shear strain for the resonant column was between 0.001% - 0.1% (small to medium shear strains) and the TRX experiments focused on the higher strains that was between 0.01% -10%.

The resonant column test equipment has a torsional drive that vibrates the top of the soil specimen in first mode resonance at different frequencies up to 250 Hz whereas the bottom is locked for any movement. The top platen monitor has some seonsor and transducer to apply and measure a torsional motion and torque. The sensor has no contact to the top platen and is able to measure rotational deformation in the sense of 10-6. Fig. 8 shows the system and the resonance frequency and amplitude of the vibration are observed, and the rate of the wave propagation along with the size of the strain are reckoned with the direction of elasticity theory (Cavallari 2016). Finally, maximum shear modulus, G_{max}, can be estimated using the shear wave velocity in the laboratory in order to constitute the soil behavior (linear or nonlinear).

The TRX test equipment consists of servo valves that provide closed-loop, electro-hydraulic and vertical motion control. With the dynamic triaxial test system, vertical load, vertical displacement, pore water pressure and volume changes can be measured. The test system is presented in Fig. 9. In order to determine the behavior of soils under dynamic loads, experiments are carried out under different ambient pressures and loadings. With the help of this test system, shear modulus and unit deformation values are

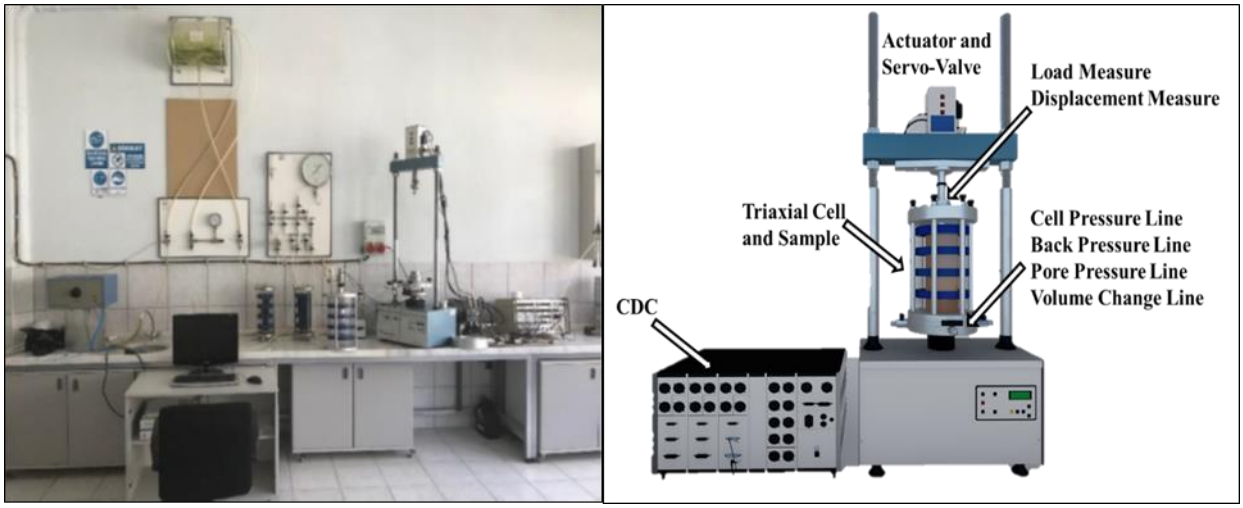

Fig. 9 Cyclic triaxial test system

Fig. 10 Undisturbed sample removed from tube

obtained with the behavior obtained at high deformation levels. Both test systems are widely used in modeling the behavior of soils in earthquake zones.

4.1 Sample preparation and testing procedures

As a result of the drilling works carried out in the studied area, undisturbed samples were obtained from 4 borings (BH-1 to 4). The depth for the BH-1 and BH-4 was about 20 m, and BH-2 and BH-3 reached a depth of 25 m. Undisturbed samples taken at every 5m were removed from the tubes in the laboratory (Fig. 10).

After removing the undisturbed samples from the tubes, samples of 70 mm x 140 mm for TRX experiments and 50 mm x 100 mm for RC experiments were prepared. In addition, the natural water content value of the samples was measured. Identification experiments were conducted by separating a certain amount from each tube and the results are presented in Table 1.

As seen in the table, fine content is very high being more than 89% for all the samples. The soil type can be defined as low to high plasticity silts and clays. Figure 11 shows the variation of the plasticity of the samples in the plasticity chart.

It is interesting to underline that most of the samples fell on the A-line with some outliers. The amount of the different soil types was found to be similar, each being 4 or 5 and half of the samples were being low plasticity and the other half high plasticity.

The undisturbed samples were placed in the cyclic triaxial experiment at the in-situ water content. A membrane was prepared with the sample placement apparatus and the sample was put inside. Filter paper and porous stone were set on the upper and lower parts of the sample. The top cap was located and then the outer cell of the experimental system was settled and filled with water. The first stage is the saturation stage that it was executed with the help of CO_2 gas and controlled by the B value being at least 0.96. Then, confining pressure was applied to the cell with the help of air pressure in the system. The confining pressure was applied differently for each depth. The consolidation process was initiated by giving the sample the confining pressure at its in-situ conditions. Finally, the samples were cyclically loaded by strain controlled tests and continued until high shear strains were recorded. The tests were conducted as strain controlled. These operations were done on all samples (Fig. 12).

Table 1 Test program

BH No	Undisturbed Sample No	Test No	Test Type	Size (mm)	Depth (m)	w_n (%)	FC (%)	Soil Type
BH-1	UD-1	1	RC-1	50*100	2.50	41.48	92.00	ML
		2	TRX-1	70*140				
	UD-2	3	RC-2	50*100	7.50	43.56	95.00	MH
		4	TRX-2	70*140				
	UD-3	5	RX-3	50*100	12.50	44.53	89.00	CH
		6	TRX-3	70*140				
	UD-4	7	RC-4	50*100	17.50	46.00	94.00	CH
		8	TRX-4	70*140				
BH-2	UD-1	9	RC-1	50*100	2.50	43.95	94.00	CL
		10	TRX-1	70*140				
	UD-2	11	RC-2	50*100	7.50	50.95	96.00	CL
		12	TRX-2	70*140				
	UD-3	13	RX-3	50*100	12.50	50.35	92.00	MH
		14	TRX-3	70*140				
	UD-4	15	RC-4	50*100	17.50	53.46	95.00	CH
		16	TRX-4	70*140				
	UD-5	17	RC-5	50*100	22.50	58.13	96.00	CH
		18	TRX-5	70*140				
BH-3	UD-1	19	RC-1	50*100	2.50	48.40	95.00	ML
		20	TRX-1	70*140				
	UD-2	21	RC-2	50*100	7.50	45.92	98.00	CL
		22	TRX-2	70*140				
	UD-3	23	RX-3	50*100	12.50	46.68	94.00	MH
		24	TRX-3	70*140				
	UD-4	25	RC-4	50*100	17.50	50.52	97.00	MH
		26	TRX-4	70*140				
	UD-5	27	RC-5	50*100	22.50	49.89	96.00	CH
		28	TRX-5	70*140				
BH-4	UD-1	29	RC-1	50*100	2.50	42.24	94.00	ML
		30	TRX-1	70*140				
	UD-2	31	RC-2	50*100	7.50	45.88	89.00	ML
		32	TRX-2	70*140				
	UD-3	33	RX-3	50*100	12.50	45.30	92.00	CL
		34	TRX-3	70*140				
	UD-4	35	RC-4	50*100	17.50	48.58	95.00	ML
		36	TRX-4	70*140				

The shear modulus was obtained at the calculated speed and density of the sample. In the test system, the angle of rotation at the top of the sample was measured with a proximeter. Placement of the sample and the equipment are shown in Fig. 13.

The samples to be used in the resonant column experiment were first trimmed to be 50 mmx100 mm in size. After the placement of the membrane, the sample was placed into the system with the help of the sample placement apparatus. The motor and proximeter were set at the top of the sample and the outer cell was installed. After the saturation and consolidation processes, shear strain values were obtained at the target confining pressure depending on the depth of the sample. These procedures were repeated for all samples (RC/Torsional Shear Testing System).

5. Results and discussion

Undisturbed samples were tested under the conditions specified in the test program. Firstly, the data obtained from the dynamic triaxial experimental system were examined. In strain-controlled experiments, the deformation was increased at each stage and 10 cycles were obtained at each

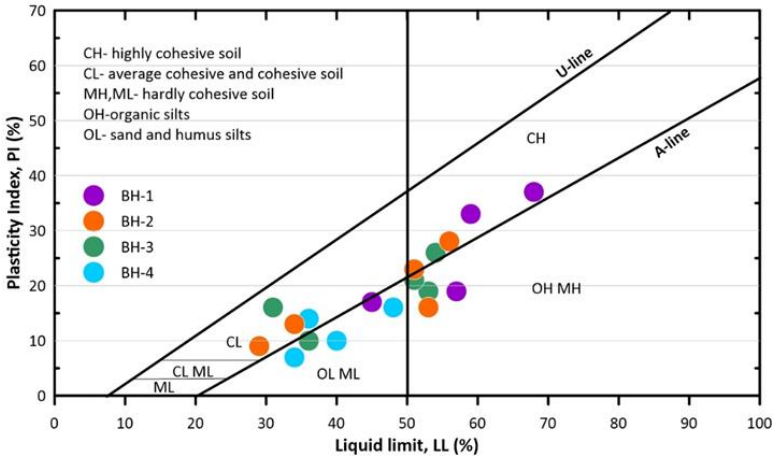

Fig. 11 Display of undisturbed samples on the plasticity chart

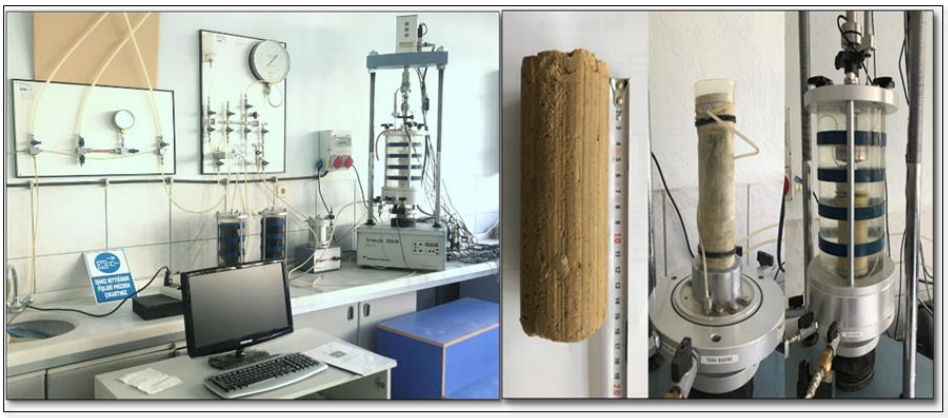

Fig. 12 Undisturbed sample and dynamic triaxial test system

Fig. 13 Undisturbed sample and resonant column test system

strain level.

Hysteresis loops were plotted using the deviator axial stress-strain data after the cyclic testing were finished. As shown in Eq.(1), the slope of the axial stress-strain hysteresis loop was calculated to derive Young's modulus.

$$E = \frac{\Delta\sigma_d}{\Delta\varepsilon_a} \quad (1)$$

$\Delta\sigma_d$= amplitude of deviator stress; and $\Delta\varepsilon_a$= amplitude of axial strain.

The shear modulus for a wide strain rate may be determined from the Young's modulus using the following equation, according to Kokusho (1980), who carried out a series of cyclic triaxial experiments.

$$G = \frac{E}{2\,(1+\nu)} \quad (2)$$

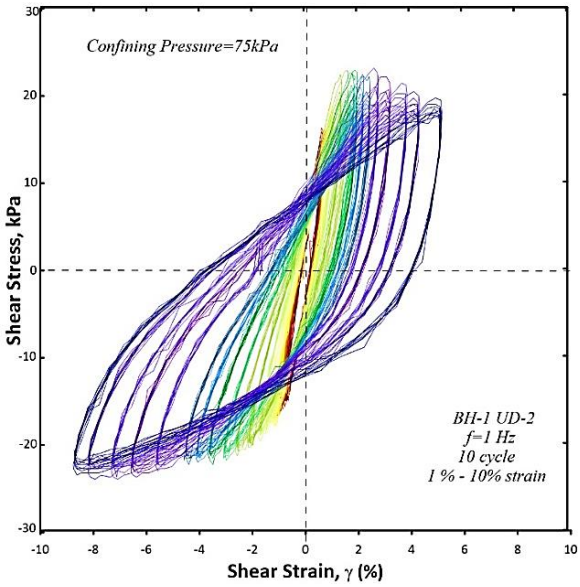

Fig. 14 Stress-strain curves of the undisturbed soil

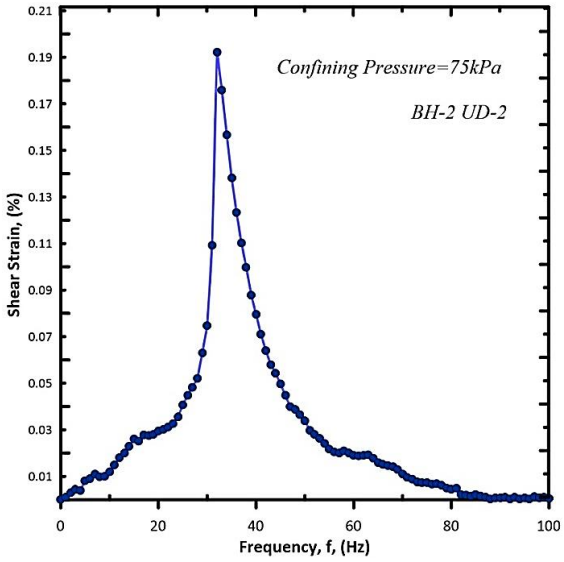

Fig. 15 Typical plot of half-power bandwidth method for BH-2 at 75 kPa

E = Young's modulus; and ν = Poisson's ratio.

Given that the shear modulus is defined as the ratio of shear stress to strain, G=Δτ/Δγ, the study used the following relationship to get the induced shear strain

$$\Delta\gamma = \Delta\varepsilon_a\,(1+\nu) \tag{3}$$

The experimental results were evaluated with these formulas (Ghayoomi *et al.* 2017, Song *et al*. 2022).

An example set of the loops belonging to the test results between 1% -10% deformation performed at 1 Hz frequency of the undisturbed sample obtained at 7.5 m from the BH-1 boring is presented in Fig. 14. Shear modulus and damping values at different shear strains were obtained from the hysteresis loops obtained for each sample.

Regarding the resonant column test system, the damping ratio values were obtained from two different methods whereas the shear modulus values were collected as a result of the torque force applied to the system. In this study, the damping ratio using half-power bandwidth method is used and the corresponding resonance frequency curve of the BH-2 boring is shown in Fig. 15. The resonance frequency was recorded as around 36 Hz for this case.

5.1 Modulus reduction behavior

As a result of dynamic experiments conducted with undisturbed samples in each borehole, the modulus reduction behavior was constructed from the loops obtained at different shear strain levels. Since the behavior consists of two different test results, it is necessary to define a transition region between being 0.1% strain. The idea of specifying this region is the to see the change in behavior

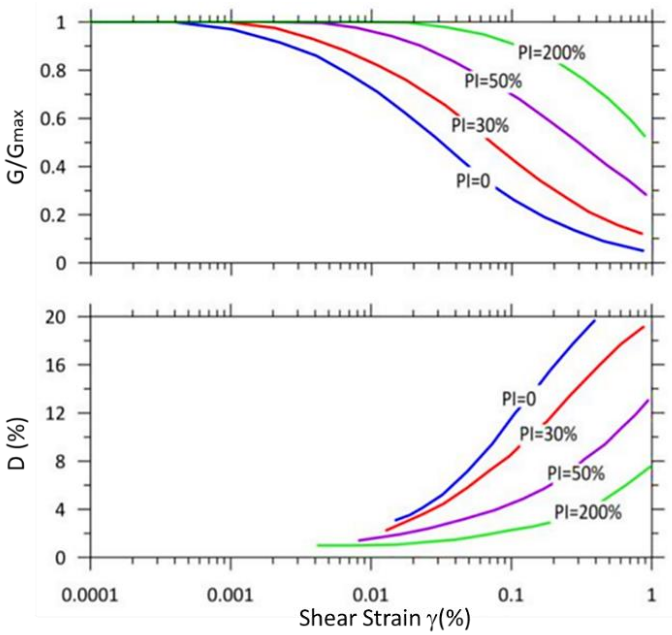

Fig. 16 Vucetic and Dobry (1991) model of different PI values (Stewart *et al*. 2014)

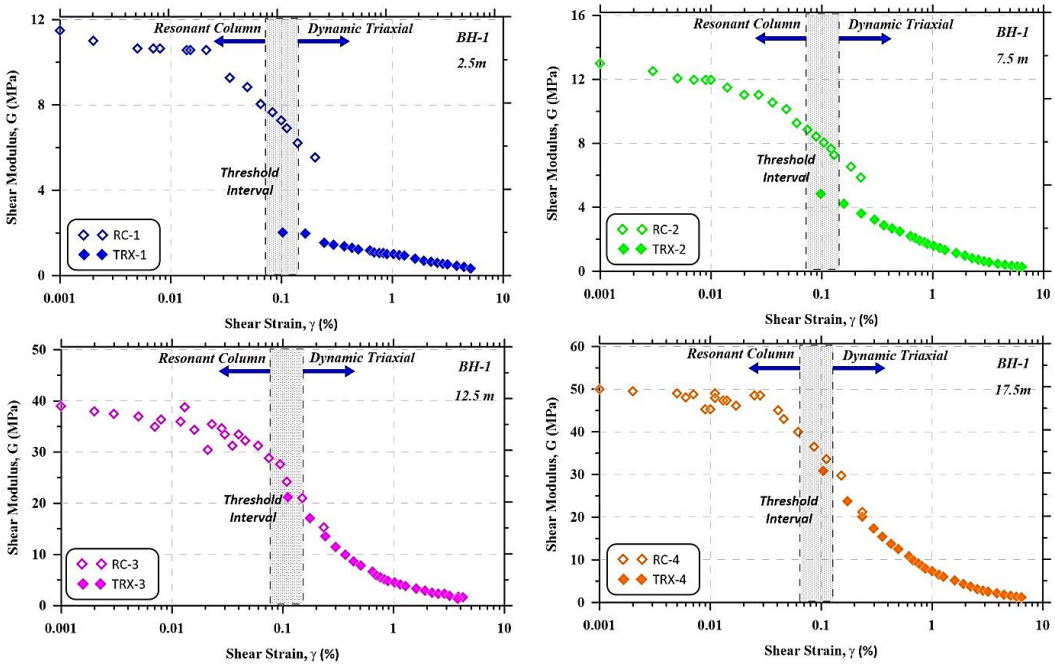

Fig. 17 Resonant column and dynamic triaxial experiment results of BH-1

through the soil column. The variation of the shear modulus over the shear strains will be presented in two parts: 1) BH-1 values will be shown to interpret the behavior at different depths and 2) The data from all the points will be discussed together.

Researchers have proposed many models that reflect the dynamic properties of soils. Among these models, Vucetic and Dobry (1991) produced a model depending on the PI value (Fig. 16), Darendeli (2001) offered a model regarding the PI, OCR, σ'_v and K_o values and finally Amir-Faryar *et al.* (2016) suggested a model related to fiber contribution in the soil sample. In order to verify the data, these models, which are widely used in the literature, were selected (Table 2).

Fig. 17 shows the behavior of the BH-1 at different depths. The initial rigidity of the soil rises as the depth increases. It is important to see that the capacity of the equipment is limited at the lower strains below 0.001%. As mentioned before, the effective stress and the PI are the prominent parameters to estimate the initial shear modulus.

The resonant column tests can measure the shear modulus up to 0.2-0.3% of shear strain levels as seen in the

Table 2 Reference model function

Shear Modulus	$\frac{G}{G_{\max}} = \frac{1}{1+\left(\frac{\gamma}{\gamma_r}\right)^a}$	*RC+TS experiments were carried out with 110 samples from 20 different areas.*	*Darendeli (2001)*
Damping ratio	$D_{Ma\sin g} = c_1 D_{Ma\sin g,a=1.0} + c_2 D_{Ma\sin g,a=1.0}{}^2 + c_3 D_{Ma\sin g,a=1.0}{}^3$, $D_{Ma\sin g,a=1.0} = \frac{1}{\Pi}\left[4\frac{\gamma - \gamma_r \ln\left(\frac{\gamma+\gamma_r}{\gamma_r}\right)}{\frac{\gamma^2}{\gamma+\gamma_r}} - 2\right]$,		
Shear Modulus	FC = 0.0% $\frac{G}{Gmax} = \frac{1}{1+6.141\gamma^{0.9122}e^{(-0.1546\gamma+0.00983\gamma^2)}}$	*Two universal mathematical models are used.*	*Amir-Faryar vd. (2016)*
Damping ratio	FC = 0% $D(\%) = \left[\left(12.13e^{0.795log_{10}\gamma}\right) \times \left(\log_{10}(\gamma+4.646)\right)^{-1.158}\right] - 0.455$		

figure. The threshold interval around 0.1% is also presented in the figure and the data signals that the shear modulus have a better consensus as the depth increases. At very shallow depths (2.5 and 7.5 m), there is a big gap for the shear modulus observed from the triaxial and resonant column tests; however, it closes down at deeper levels. Tests are customarily conducted at around 100 kPa (1 atm) and it may not be pointed out before that the shear modulus observed at this transition region is questionable at the depths close to the ground surface. On the other hand, two tests are in a harmony at the threshold strain interval at higher depths, especially over 1 atm.

It was expected to see that the G_{max} values increased depending on the depth. Regarding the BH-1 boring, there was a sudden rise after 10-15 m depth. The soil changes to ML-MH to CH at that depth along with the change in PI from 17-19% to 33-37%. The variation is not that high for other borings. Examining the results of the experiments on undisturbed samples at 15-20 m depth solely, it was seen that the G_{max} of BH-1 with PI of 37% almost 4 times bigger than the rest with the PI value of 20% in average. The effect of PI value along with the effective stress on the change of G_{max} values was clearly observed.

Shear wave velocity measurement (V_s) was measured at the points where boreholes exist. V_s values obtained from resonant column experiments were compared with the seismic measurements performed in the field. The model has the R^2 = 0.9158 given a good relation between the values and it is presented in Fig. 18.

In addition, G_{max} values obtained in the laboratory and Vs values obtained from the field were compared with the data obtained in the formula $G_{max} = \rho.V_s^2$. Regarding the data, when in situ and laboratory measurements were compared, it was determined as R^2=0.9475.

Experiment results were compared with three reference models commonly used in the literature according to depths in order to evaluate and examine their accuracy. Vucetic and Dobry (1991), Darendeli (2001) and Amir-Faryar *et al.* (2016). The results were evaluated with the reference curves proposed.

The observed normalized shear modulus data from the 36 dynamic tests including the literature models are exhibited in Fig. 19. It should be noted that the PI value was averaged to calculate the reference curves. The TRX data falls in between the Vucetic and Dobry (1991) and Darendeli (2001) models whereas, the RC data follows Amir-Faryar *et al.* (2016) model mostly with some outliers at 0-5 m depth. For the higher depth of 5-10 m, the data at low strain levels have a very good match with the Amir-Faryar *et al.* (2016) curve while it is obvious that the shear modulus data followed the Vucetic and Dobry curve at high strain levels.

At the levels from 10m-20 m, the TRX results have a great agreement with Vucetic and Dobry (1991) and Amir-Faryar *et al.* (2016) models as the Darendeli model stayed below being on the conservative side. The reason for that is the model offered from Darendeli (2001) is the average model constructed on a big data. The upper limit of the data

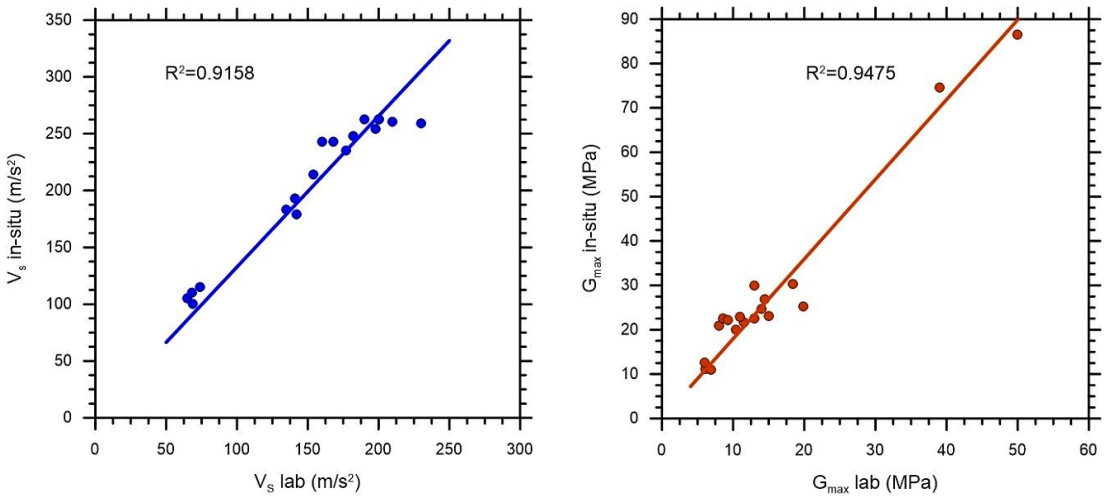

Fig. 18 Comparison of in-situ and laboratory measurements

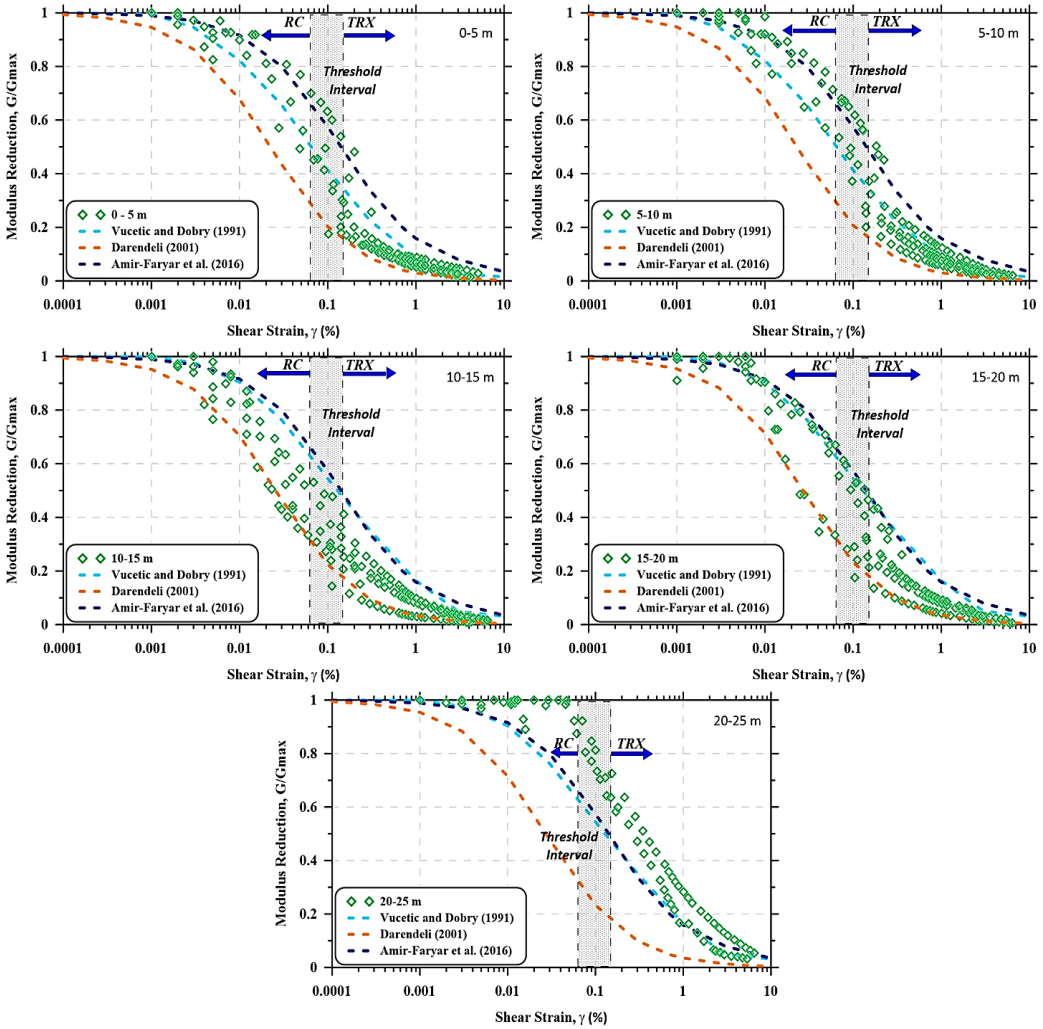

Fig. 19 Comparison of all shear modulus reduction values with reference curves

presented in his thesis have a good match with the data presented here. The RC data is a bit over the reference curves although it fairly tracks the Vucetic and Dobry and Amir-Faryar *et al*. (2016) models. It is interesting to see a good match on TRX data with the literature but overestimation of the RC data compared to the reference curves.

There are only two undisturbed samples taken from the

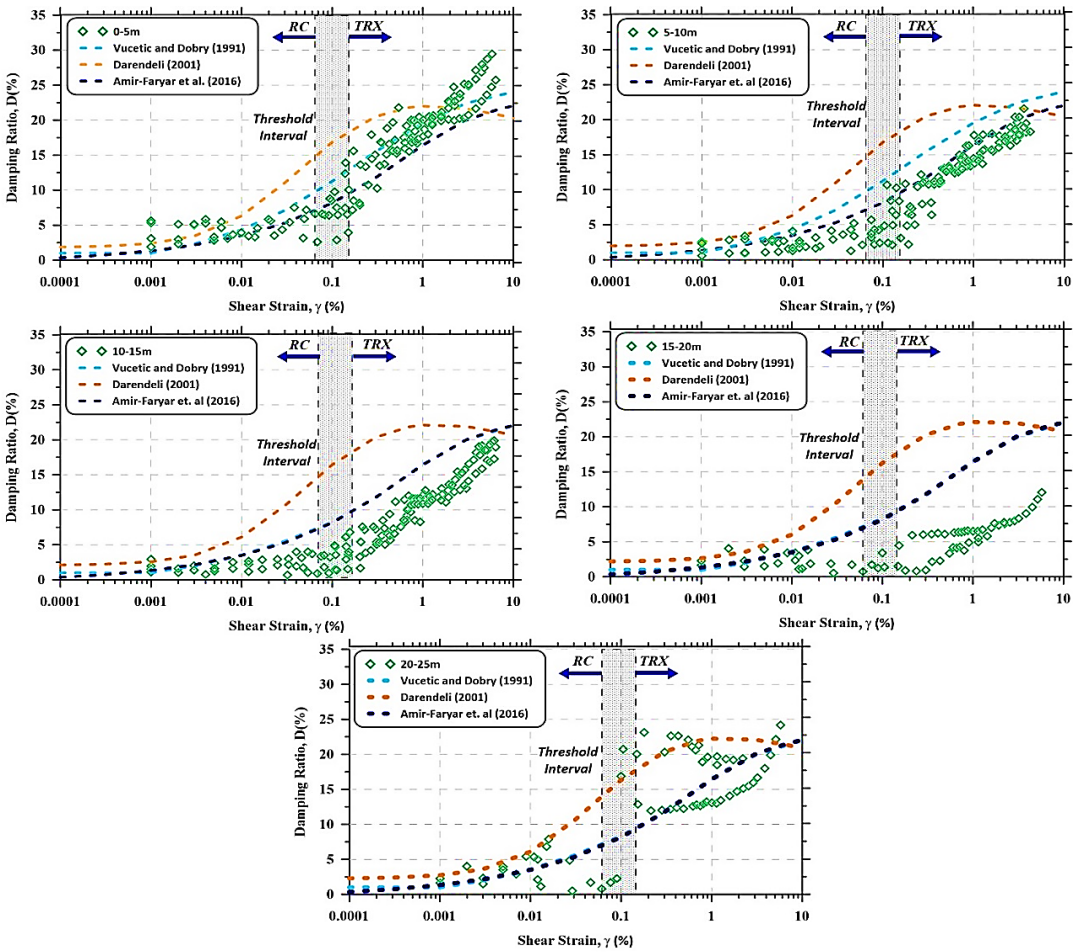

Fig. 20 Comparison of all damping ratio values with reference curves

boring at 20-25 m depths therefore it is not that clear to come up some conclusions. However, both data showed that none of the reference curves are good to match with the test results. It is believed that none of the models were constructed for the high confining pressure levels therefore there is a bit difference between the models and the reference curves.

5.2 Damping behavior

Another important parameter underlying the dynamic behavior is the damping ratio over the shear strain. It shows the capacity of the absorbed energy to be able to finish the cycle. Damping values of the dynamic experiments were extracted from the loops and the variation over a wide strain range is presented in Fig. 20. It has been observed in the literature that the damping values are more scattered compared to the shear modulus values. As seen in the very shallow depths, the data is distributed over a larger range.

The data showed similar behavior with reference curves between 0.001% and 0.01%, and results were lower than the reference curves for strain values greater than 0.01%. After the transition zone, the tendency follows the Amir-Faryar *et al.* (2016) model and falls on to the Vucetic and Dobry (2001) model at higher shear strains being over the reference curves.

Investigating the depth of 5-10 m, it is seen that some points were a bit lower even though the data over all is close to the reference curve of Amir-Faryar *et al.* (2016) especially after the threshold interval. It is a clear point that the initial part overestimated by the models or at least the RC test data is not compatible with the curves as much.

For the reference curves at the depth of 10-15 m and lower, it is seen that Vucetic and Dobry (1991) and Amir-Faryar *et al.* (2016) show similar behavior. It is seen that RC and TRX test results are staying below compared to the reference curves and the difference increases with the rise in confining pressure. It can be seen that reference curves are generally observed at large deformation levels.

The damping values are way dispersed in comparison to the lower depths for the data observed from 15-25 m levels. It is one obvious point is that a clear interpretation cannot be made due to the low values and the scattered data of the damping values at deeper levels.

5.3 General normalised shear modulus and damping ratio models

The data obtained as a result of the experiments were compared with the liter models and evaluations were made. Then all the data were combined. Data are limited to upper limit, lower limit and fitting curves and are shown in Figs. 21 and 22.

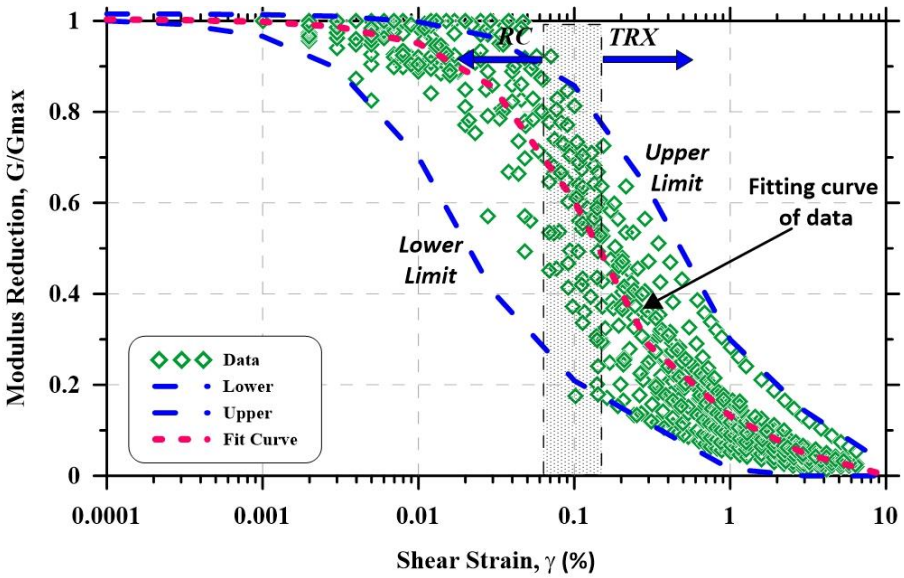

Fig. 21 The model curve that best fitting the data for modulus reduction

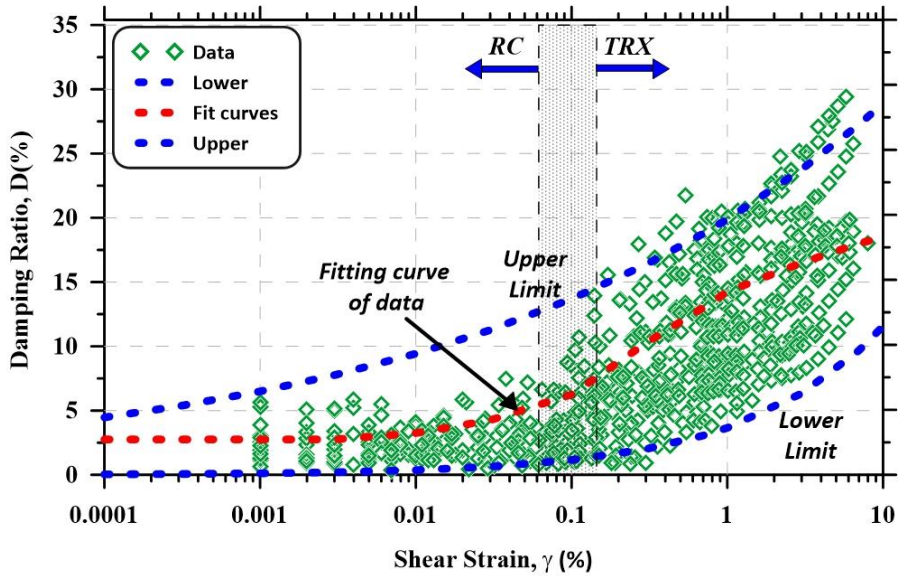

Fig. 22 The model curve that best fitting the data for damping ratio

For the reliability of the models, the correlation coefficient 'R' and the definition coefficient 'R^2' are given. The closer this value is to 1.0, the higher the reliability of the model. If the R value is greater than 0.8, there is a good relationship between the two variables, whereas if it is less than 0.5, there is a weak relationship. After combining the data with the help of MATLAB® software, the suggested models for these three limits were obtained.

As a result of the analyzes made, the definition coefficient in the modulus reduction model recommended for clay samples between 0-50kPa for the lower limit is 0.9966. The damping values of this curve are 0.9727. When examined as the upper limit, an identification coefficient of 0.9968 was obtained in the modulus reduction model for samples between 200-250kPa, and 0.9261 in the damping value.

After the experiments and evaluation of the data, the original proposed model was obtained as 0.944 in the modulus reduction model for ambient pressures between 50-200kPa, and as 0.641 for the damping curve. The formulas and definition coefficients of these models are shown in Table 3.

6. Conclusions

The behavior of soils under dynamic loads is of great importance in the geotechnical and structural engineering fields. In order to design the structures both more safely and economically, the soil behavior at the ground surface should be estimated correctly as to take it into account for the.

In this study, undisturbed soil samples were taken from

Table 3 General normalised shear modulus and damping ratio models

Modulus Reduction (G/G_{max}) ***RC+TRX experiments (36) were carried out with undisturbed samples under different confining pressure* conditions.**	*Lower* *(For clay PI:7-37, Confining Pres.:0-50kPa)*	**General model:** $\frac{G}{G_{max}} = 0.7296*exp(-52.01*\gamma) + 0.2743*exp(-2.894*\gamma)$ Coefficients (with 95% confidence bounds): R-square: 0.9966 Adjusted R-square: 0.9952
	Mean *(For clay PI:7-37, Confining Pres.:50-200kPa)*	**General model:** $\frac{G}{G_{max}} = 0.7911*exp(-6.776*\gamma) + 0.2124*exp(-0.4891*\gamma)$ Coefficients (with 95% confidence bounds): R-square: 0.944 Adjusted R-square: 0.9437
	Upper *(For clay PI:7-37, Confining Pres.:200-250kPa)*	**General model:** $\frac{G}{G_{max}} = 0.7224*exp(-2.348*\gamma) + 0.2931*exp(-0.2406*\gamma)$ Coefficients (with 95% confidence bounds): R-square: 0.9968 Adjusted R-square: 0.9954
Damping ratio (D,%) ***RC+TRX experiments (36) were carried out with undisturbed samples under different confining pressure conditions.***	*Lower* *(For clay PI:7-37, Confining Pres.:0-50kPa)*	**General model:** $D = 3.656*\gamma^{(0.5002)}$ Coefficients (with 95% confidence bounds): R-square: 0.9727 Adjusted R-square: 0.9702
	Mean *(For clay PI:7-37, Confining Pres.:50-200kPa)*	**General model:** $D = 11.69*\gamma^{(0.3242)}$ Coefficients (with 95% confidence bounds): R-square: 0.641 Adjusted R-square: 0.6405
	Upper *(For clay PI:7-37, Confining Pres.:200-250kPa)*	**General model:** $D = 19.89*\gamma^{(0.1621)}$ Coefficients (with 95% confidence bounds): R-square: 0.9261 Adjusted R-square: 0.922

different borings near one of the Turkey's major faults and resonant column dynamic characteristics (RC) and dynamic triaxial (TRX) tests were performed to determine the dynamic behavior of the soil. The obtained results are presented as follows:

• The laboratory V_s values obtained from the RC experimental system and the values obtained from the field were compared and it was found that an R^2 of 0.9158. The G_{max} was calculated with the V_s values taken from the field and it was compared with values gained from the RC tests

in the laboratory. It was noted that an R^2 of 0.9475.

• A transition zone is defined around 0.1% where the results of the RC-TRX tests performed on the undisturbed samples are combined. It is seen that the shear modulus of the samples in this region do not match at shallow depths having a big gap whereas the differences between the TRX and RC shear modulus disappear as the confining pressure increases, especially over 100 kPa.

• The tests were conducted at every 5m and the observed shear modulus and damping behavior are compared with the reference curves widely used in the literature. The results showed that the data is generally compatible with the reference curves but some difference was noticed at higher depths.

• After evaluating the accuracy of the test results, three modulus reduction models and damping curves are proposed to be evaluated at different confined pressures.

It is considered that these models can be used for similar soils due to the cost and time-consuming to find the dynamic parameters of the soils through the laboratory testing.

Declaration of competing interest

The authors declare that they have no known competing financial interests or personal relationships that could have appeared to influence the work reported in this paper.

Acknowledgments

This work has been supported by Eskisehir Osmangazi University Scientific Research Projects Coordination Unit under grant number: 201915A211

This study was conducted by Ersin Güler at the Institute of Natural and Applied Science of Eskişehir Osmangazi University as a Ph.D. thesis.

References

Amir-Faryar, B., Aggour, M.S. and McCuen, R.H. (2017), "Universal model forms for predicting the shear modulus and material damping of soils", *Geomech. Geoeng*., **12**, 60-71 https://doi.org/10.1080/17486025.2016.1162332

Akbaş, B., Akdeniz, N., Aksay, A., Altun, İ.E.., Balcı, V., Bilginer, E, Bilgiç, T., Duru, M., Ercan, T., Gedik, İ., Günay, Y., Güven, İ.H., Hakyemez, H.Y., Konak, N., Papak, İ., Pehlivan, Ş., Sevin, M., Şenel, M., Tarhan, N., Turhan, N., Türkecan, A., Ulu, Ü., Uğuz, M.F., Yurtsever, A., *et al*. (2002), prepared by the Geological Research Department of the General Directoate of Mineral Research and Exploration, produced by ISLEM Geographic Information Systems Company in ARC/INFO 8.1 encüviroment, 2002 and printed by General Command of Mapping. Topographic information is taken by modifying from the 1:500.000 and 1:250.000 scale topographic maps (projection system is Lambert Conformal Conic) of General Command of Mapping (Ankara).

ASTM. D4015-15. Standard test methods for modulus and damping of soils by resonant-column method. D4015-15.

ASTM D4767-11. Standard Test Method for Consolidated Undrained Triaxial Compression Test for Cohesive Soils, Annual Book of ASTM Standards, 913-925.

Bayat, M. and Ghalandarzadeh, A. (2018), "Stiffness degradation and damping ratio of sand-gravel mixtures under saturated state". *Int. J. Civ. Eng*., **16**, 1261-1277. https://doi.org/10.1007/s40999-017-0274-8.

Bol, E. (2003), "Geotechnical properties of Adapazarı soils", Ph.D. Thesis. Sakarya Üniversitesi Natural and Applied Sciences.

Boğaziçi University Kandilli Observatory and Earthquake Research Institute Regional Earthquake-Tsunami Monitoring Center. Seismicity Map for (2020), http://www.koeri.boun.edu.tr/sismo/2/depremverileri/depremselik-haritalari/

Cavallari, A. (2016), "Resonant column testing challenges". 1st IMEKO TC-4 International Workshop on Metrology for Geotechnics Benevento, March 17-18, Italy.

Chattaraj, R. and Sengupta, A, (2016), "Liquefaction potential and strain dependent dynamic properties of Kasai River sand", *Soil Dyn. Earthq. Eng*., **90**, 467-475, https://doi.org/10.1016/j.soildyn.2016.07.023

Darendeli, M.B. (2001), "Development of a new family of normalized modulus reduction and material damping curves", Ph.D. Thesis. The University of Texas at Austin, ABD.

Ghayoomi, M., Suprunenko, G. and Mirshekari, M. (2017), "Cyclic triaxial test to measure strain-dependent shear modulus of unsaturated sand", *Int. J. Geomech*., **17**(9). https://doi.org/10.1061/(ASCE)GM.1943-5622.0000917.

Güler, E. and Afacan, KB. (2021), "Dynamic behavior of clayey sand over a wide range using dynamic triaxial and resonant column tests". *Geomech. Eng*., 105-113. https://doi.org/10.12989/gae.2021.24.2.105.

Harman, E. and Küyük, HS. (2016), "Probabilistic seismic hazard analysis for the city of Sakarya", *J. SAU*, **20**, 23-31.

Houbrechts, J., Schevenel, M., Lombaert, G., Degrande, G., Rucker, W., Cuellar, V. *et al*. (2011), "RIVAS WP1.1. Test procedures for the determination of the dynamic soil characteristics", 1-107.

Hussain, M. and Sachan, A., (2019), "Dynamic characteristics of natural kutch sandy soils", *Soil Dyn. Earthq. Eng*., **125**, 105717. https://doi.org/10.1016/j.soildyn.2019.105717.

Jamali, H., Tolooiyan, A., Dehghani, M., Asakereh, A. and Kalantari, B. (2018), "Post-long-term cyclic behaviour of Coode Island Silt (CIS) containing different sand content", *Appl. Ocean Res*., **80**, 11-23. https://doi.org/10.1016/j.apor.2018.08.018.

Kaya, Z. and Erken, A. (2015), "Cyclic and post-cyclic monotonic behavior of Adapazari soils", *Soil Dyn. Earthq. Eng*., **77**, 83-96 https://doi.org/10.1016/j.soildyn.2015.05.003

Ketin, İ. (1991), The North Anatolian Fault. Journal of MTA.

Kim, A.R., Chang, I., Cho, G.C. and Shim, S.H. (2018), "Strength and dynamic properties of cement-mixed Korean marine clays". *KSCE J. Civ. Eng*., **22**, 1150-1161. https://doi.org/10.1007/s12205-017-1686-3.

Kokusho, T. (1980), "Cyclic triaxial test of dynamic soil properties for wide strain range", *Soils Found*., **20**, 45-60. https://doi.org/10.3208/sandf1972.20.2_45.

Komazawa, M., Morikawa, H., Nakamura, K., Akamatsu, J., Nishimura, K., Sawada, S., Erken, A. and Önalp, A. (2002), "Bedrock structure in Adapazari, Turkey – A possible cause of severe damage by the 1999 Kocaeli Earthquake", *Soil Dny. Earthq. Eng*., **22**, 829-836.

Kumar, S.S., Krishna, A.M. and Dey, A. (2017), "Evaluation of dynamic properties of sandy soil at high cyclic strains", *Soil Dyn. Earthq. Eng*., **99**, 157-167. https://doi.org/10.1016/j.soildyn.2017.05.016.

Kweon, G.C. and Kim, D.S. (2000), "Deformational characteristics of subgrade soils in Korea", *KSCE J. Civ. Eng*., **4**, 83-90. https://doi.org/10.1007/bf02830821.

Li, H. and Senetakis, K. (2018), "Effects of particle grading and stress state on strain-nonlinearity of shear modulus and damping ratio of sand evaluated by resonant-column testing", *J. Earthq. Eng*., 1-27. https://doi.org/10.1080/13632469.2018.1487349.

Park, C.S., Park, I.B. and Mok, Y.J. (2015), "Evaluation of resilient moduli for recycled crushed-rock-soil-mixtures using in-situ seismic techniques and large-scale resonant column tests", *KSCE J. Civ. Eng*., **19**, 1647-1655. https://doi.org/10.1007/s12205-014-1020-2.

RC/Torsional Shear Testing System. GCTS Testing. Resonant Column/Torsional Shear Testing System and CATS Module.

Sakarya Governorship Provincial Directorate Of Environment And Urbanization (2018), Sakarya Province 2017 Environmental Status Report.

Salem, M.A., Karim, A.M. and El-Sherbini, E.A. (2018), "Static and dynamic properties of cohesionless soil–new Suez canal area–Ismailia–Egypt", *Int. J. Geotech. Eng*., 1-12 https://doi.org/10.1080/19386362.2018.1514756

Sexena, S.K. and Reddy, K.R. (1989), "Dynamic moduli and damping ratios for monterey no.0 sand by resonant column tests", *Soils Found*., **29**(2), 37-51. https://doi.org/10.3208/sandf1972.29.2_37.

Shivaprakash, B.G. and Dinesh, S.V. (2018), "Effect of plastic fines on initial shear modulus of sand-clay mixtures", *KSCE J. Civ. Eng*., **22**, 73-82. https://doi.org/10.1007/s12205-017-1076-x

Sobolev, E. and Ter-Martirosyan, A. (2018), "Interaction of the base and construction under seismic action, with considering various characteristics of soil damping", MATEC Web Conf, 251. https://doi.org/10.1051/matecconf/201825104011.

Song, D., Liu, H. and Sun, Q., (2022), "Significance of determination methods on shear modulus measurements of Fujian sand in cyclic triaxial testing", *Appl. Sci*., **12**(8690). https://doi.org/10.3390/app12178690

Stewart, J.P., Afshari, K. and Hashash, Y.M.A. (2014), "Guidelines for performing hazard-consistent one-dimensional ground response analysis for ground motion prediction", Report PEER. **16**, 152.

Subramaniam, P. and Banerjee, S. (2016), "Torsional shear and resonant column tests on cement treated marine clay", *Indian Geotech. J.*, **46**, 183-191. https://doi.org/10.1007/s40098-015-0170-6

Thomas, G. and Rangaswamy, K. (2020), "Dynamic soil properties of nanoparticles and bioenzyme treated soft clay", *Soil Dyn. Earthq. Eng*., **137**, 106324. https://doi.org/10.1016/j.soildyn.2020.106324

Varghese, R., Senthen Amuthan, M., Boominathan, A. and Banerjee, S. (2019), "Cyclic and postcyclic behaviour of silts and silty sands from the Indo Gangetic Plain", *Soil Dyn. Earthq. Eng*., **125**, 105750. https://doi.org/10.1016/j.soildyn.2019.105750.

Vucetic, M. and Dobry, R. (1991), "Effect of soil plasticity on cyclic response", *ASCE J. Geotech. Eng*., **117**(1), 89-107.

Zhou, W., Chen, Y., Ma, G., Yang, L. and Chang, X. (2017), "A modified dynamic shear modulus model for rockfill materials under a wide range of shear strain amplitudes", *Soil Dyn. Earthq. Eng*., **92**, 229-238. https://doi.org/10.1016/j.soildyn.2016.10.027